lpve
land product validation and evolution
European Space Agency

Calibration and Validation of land surface temperature for Landsat8-TIRS sensor

***D. Skoković[1], J.A. Sobrino[1], J.C. Jiménez-Muñoz[1], G. Sòria[1], Y. Julien[1], C. Mattar[2] and* Jordi Cristóbal[3]**

[1]*Global Change Unit, IPL-University of Valencia (Spain)* [drazen.skokovic@uv.es]
[2]*Laboratory for Analysis of the Biosphere, University of Chile (Chile)*
[3]*Geophysical Institute, University of Alaska (USA)*

INTRODUCTION

TIRS LANDSAT-8 CHARACTERISTICS

ALGORITHMS:

- **NDVI Thresholds Method**
- **Radiative Transfer Equation**
- **GAPRI database**
- **Single-Channel (SC)**
- **Split-Window (SW)**
- **Test from independent simulated data**

STUDY AREA AND DATA

RESULTS

- **Vicarious calibration**
- **Intercomparison of algorithms**

CONCLUSIONS

INTRODUCTION

- Landsat-8 satellite was launched in February-2013 ensuring the continuity of remote sensing data at high spatial resolution in the Landsat Data Continuity Mission, LDCM.

- Landsat-8 carries two sensors:
  - Operational Land Imager (OLI)
    - Spatial resolution of 30 m
    - 8 bands in the Visible and Near-Infrared (VNIR) and in the Short-Wave Infrared (SWIR) regions.
  - Thermal Infrared (TIR)
    - Spatial resolution of 100 m
    - 2 bands located in the atmospheric window between 10-12 μm

- Thermal imaging was initially excluded from the LDCM requirements.

- The increase of applications using Landsat5 TM or Landsat7 ETM+ thermal data in recent years was a key factor to finally include a TIR sensor as a part of LDCM.

- In particular, Land Surface Temperature (LST) is a key variable to be

RS LANDSAT8 CHARACTERISTICS

Platform	Sensor	Band	BW (μm)	λ_{eff} (μm)	GSD (m)
Landsat4	TM	6	10.4-12.5	11.154	120
Landsat5	TM	6	10.4-12.5	11.457	120
Landsat7	ETM+	6	10-12.5	11.269	60
Landsat8	TIRS	1	10.3-11.3	10.904	100
Landsat8	TIRS	2	11.5-12.5	12.003	100

- Lower spatial resolution than ETM+ thermal band.
- The Noise Equivalent Delta Temperature (NEΔT) is similar to the NEΔT of the previous TM sensors (0.4 K).
- First in the Landsat series that incorporate two TIR bands in the atmospheric window between 10-12 μm.

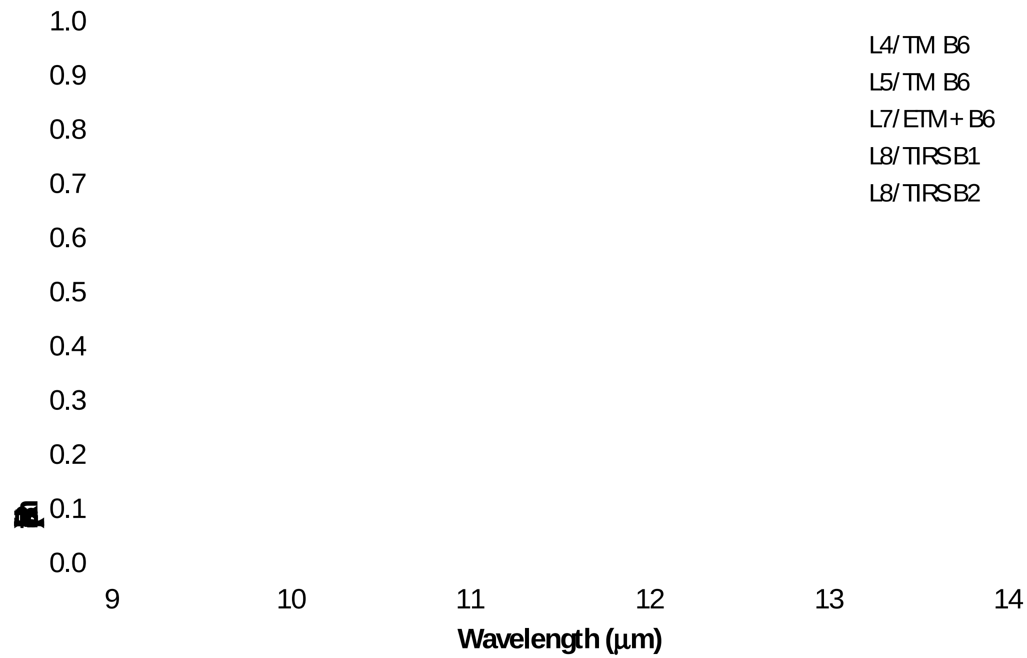

ALGORITHMS

For retrieving Land Surface Emissivity (LSE):

- NDVI Thresholds Method (NDVI-THM)
  Sobrino et al. (2008)

For retrieving Land Surface Temperature (LST):

- Radiative Transfer Equation (RTE)
- Single-Channel (SC) algorithm
  Jiménez-Muñoz et al. (2009)
- Split-Window (SW) algorithm
  Mathematical structure proposed by Sobrino et al. (1996)
  Applied to different Earth Observation sensors in Jiménez-Muñoz and Sobrino (2008)
- Global Atmospheric Profiles from Reanalysis Information (GAPRI) database
  Mattar et al. (2014)

ALGORITHMS

NDVI Thresholds Method

LSE is estimated from information collected by OLI in VNIR bands (reflectances or vegetation indices) depending on the Fractional Vegetation Cover (FVC) for a given pixel. Sobrino et al. (2008)

$$\varepsilon = a + b\rho_{red} \quad (FVC = 0)$$

$$\varepsilon = \varepsilon_s(1 - FVC) + \varepsilon_v FVC \quad (0 < FVC < 1)$$

$$\varepsilon = 0.99 \quad (FVC = 1)$$

$$FVC = \frac{NDVI - NDVIs}{NDVIv - NDVIs}$$

ρ_{red}: Reflectance in the red band (band 4)

ε_S and ε_V: Soil and vegetation emissivity values

Linear Relationship between ε and ρ_{red}

Knowing type of soil ε_S and ε_v were retrieved with ASTER spectral library

Land Cover	Band	Expression
FVC=0	TIRS-1	$0.979-0.046r_{OLI,B4}$
	TIRS-2	$0.982-0.027r_{OLI,B4}$
0<FVC≤1	TIRS-1	0.971(1-FVC)+0.987FVC
	TIRS-2	0.977(1-FVC)+0.989FVC
Water	TIRS-1	0.991
	TIRS-2	0.986
Snow/Ice	TIRS-1	0.986
	TIRS-2	0.959

ALGORITHMS

Radiative Transfer Equation (RTE)

With the thermal radiance measured at-sensor level and the atmospheric parameters obtained with radiosounding, a LST can be retrieved.

$$L_{sen} = \left[\varepsilon B_{T_S} + (1-\varepsilon)L_d\right]\tau + L_u$$

Applying the inverse of the Planck's law

$$\boxed{T_S = \frac{c_2}{\lambda \ln\left\{\dfrac{c_1}{\lambda^5\left[\dfrac{L_{sen} - L_u - \tau(1-\varepsilon)L_d}{\tau\varepsilon}\right]} + 1\right\}}}$$

$c_1 = 1.19104 \cdot 10^8$ W·µm^4·m^{-2}·sr^{-1}

$c_2 = 14387.7$ µm·K

L_{sen}: Thermal radiance at sensor level

B_{T_S}: Radiance of Planck's law

T_S: Land surface temperature

ε: Land Surface Emissivity (LSE)

τ: Atmospheric transmissivity

L_u: Up-welling atmospheric radiance

L_d: Down-welling atmospheric radiance

λ: Effective band wavelength

ALGORITHMS

Single-Channel (SC) algorithm

The practical approach proposed in the SC algorithm consists of the approximation of the atmospheric functions defined by Ψ_1, Ψ_2, Ψ_3 versus the atmospheric water vapour content W from a second order polynomial fit.

$$T_s = \gamma\left[\frac{1}{\varepsilon}\left(\psi_1 L_{sen} + \psi_2\right) + \psi_3\right] + \delta$$

- Can be applied to any of the two TIRS bands. (Preferably to TIRS 1)
- Only requires the knowledge of *w*.

Jiménez-Muñoz et al. (2009)

$$\gamma \approx \frac{T_{sen}^2}{b_\gamma L_{sen}} \qquad \psi_1 = \frac{1}{\tau}; \quad \psi_2 = -L_d - \frac{L_u}{\tau}; \quad \psi_3 = L_d$$

$$\delta \approx T_{sen} - \frac{T_{sen}^2}{b_\gamma}$$

$$\begin{bmatrix} \psi_1 \\ \psi_2 \\ \psi_3 \end{bmatrix} = \begin{bmatrix} c_{11} & c_{12} & c_{13} \\ c_{21} & c_{22} & c_{23} \\ c_{31} & c_{32} & c_{33} \end{bmatrix} \begin{bmatrix} w^2 \\ w \\ 1 \end{bmatrix}$$

$$C = \begin{bmatrix} 0.04019 & 0.02916 & 1.01523 \\ -0.38333 & -1.50294 & 0.20324 \\ 0.00918 & 1.36072 & -0.27514 \end{bmatrix}$$

$\boldsymbol{L_{sen}}$: Thermal radiance at sensor level

$\boldsymbol{T_S}$: Land surface temperature

$\boldsymbol{T_{sen}}$: At-sensor brightness temperature

$\boldsymbol{b_\gamma}$: (1324 K for TIRS-1, and 1199 K for TIRS-2)

$\boldsymbol{\Psi_1, \Psi_2, \Psi_3}$: Atmospheric functions

$\boldsymbol{w}$: Water vapour (Radiosoundings, MOD07, in situ data…)

ALGORITHMS

Split-Window (SW) algorithm

The basis of the technique is that the radiance attenuation for atmospheric absorption is proportional to the radiance difference of simultaneous measurements at two different wavelengths. Sobrino et al. (1996)

$$T_s = T_i + c_1(T_i - T_j) + c_2(T_i - T_j)^2 + c_0 + (c_3 + c_4 w)(1 - \varepsilon) + (c_5 + c_6 w)\Delta\varepsilon$$

Emissivity's extracted from ASTER spectral library

$\varepsilon = 0.5\,(\varepsilon_i + \varepsilon_j)$ $\Delta\varepsilon = (\varepsilon_i - \varepsilon_j)$

c_0 = -0.268; c_1 = 1.378; c_2 = 0.183; c_3 = 54.30; c_4 = -2.238; c_5 = -129.20 ; c_6 = 16.40

$\boldsymbol{T_S}$: Land surface temperature

$\boldsymbol{T_i}, \boldsymbol{T_j}$: At-sensor brightness temperature at bands *i* and *j*

ALGORITHM SENSITIVITY ANALYSIS (K)	
δ_{alg}	0.6
$\delta_{NE\Delta T}$	1.5 (0.4)
δ_{ε}	0.6
δ_{w}	0.1

e(LST) = 2.1 (1.5)

- The Split-Window technique uses two TIR bands typically located in the atmospheric window between 10 and 12 µm
- Similar to the SC algorithm, the SW algorithm only requires the knowledge of *w.*

ALGORITHMS

GAPRI database

Mattar, C., Durán-Alarcón, C., Jiménez-Muñoz, J. C., & Sobrino, J. A. (2013). Global Atmospheric Profiles derived from Reanalysis Information (GAPRI). IEEE Transactions on Geoscience and Remote Sensing (submitted).

Global Atmospheric Profiles from Reanalysis Information (GAPRI)

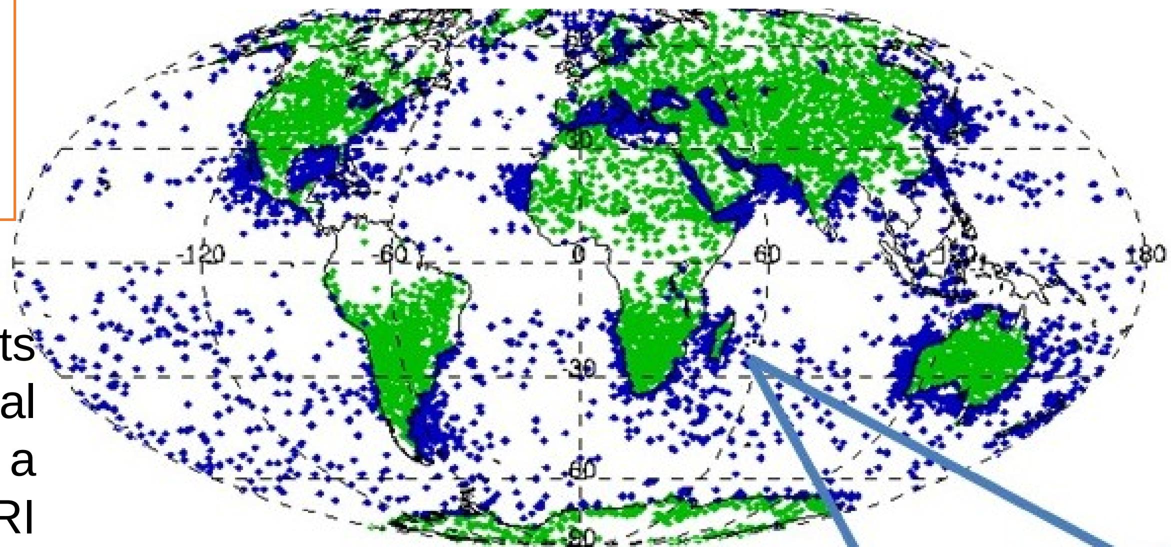

SC and SW coefficients retrieved from statistical fits performed over a simulated GAPRI database

- ERA-interim data set
- 0.75° x 0.75° spatial grid
- 29 mandatory levels
- MODTRAN format
- 4,838 atmospheric profiles
- Tropical, mid-latitude, sub-artic and artic weather conditions

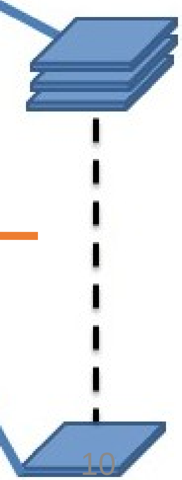

ALGORITHMS

Test from independent simulated data

Testing from independent simulated data:

- Atmospheric profiles databases
- 108 emissivity spectra (ASTER

Thermodynamic Initial Guess Retrieval (TIGRs)
STanDard atmospheres in MODTRAN (STD)

Database	Algorithm	W range ($g \cdot cm^{-2}$)	n data	Bias (K)	St. D (K)	(K)	
$TIGR_{61}$	SW	0-6	32940	-0.1	1.2	1.2	0.997
	SC	0-6	32940	-2.7	3.0	4.0	0.982
	SC	0-3	17820	-1.2	1.5	1.9	0.996
	SC	3-6	15120	-4.5	3.2	5.6	0.954
$TIGR_{1761}$	SW	0-6	950940	0.0	0.6	0.6	0.999
	SC	0-6	950940	-1.1	1.7	2.0	0.996
	SC	0-3	886680	-0.8	0.9	1.2	0.999
	SC	3-6	58860	-4.0	3.5	5.4	0.957
$TIGR_{2311}$	SW	0-6	249588	0.4	1.0	1.1	0.999
	SC	0-6	249588	-2.2	3.7	4.3	0.981
	SC	0-3	186732	-1.0	1.1	1.5	0.998
	SC	3-6	54216	-4.5	4.6	6.5	0.936
STD_{66}	SW	0-6	35640	-0.2	0.9	0.9	0.998
	SC	0-6	35640	-2.1	2.6	3.3	0.989
	SC	0-3	28080	-1.2	1.2	1.7	0.997
	SC	3-6	7020	-4.7	2.3	5.4	0.961

The sub index refers to the number of atmospheric profiles included in each database

ALGORITHMS

Testing from independent simulated data

Testing from independent simulated data

- TIGRs and STD databases
- 108 emissivity spectra (ASTER library)

Database	Algorithm	W range ($g·cm^{-2}$)	n data	Bias (K)	St. Dev. (K)	RMSE (K)	r
$TIGR_{61}$	SW	0-6	32940	-0.1	1.2	1.2	0.997
	SC	0-6	32940	-2.7	3.0	4.0	0.982
	SC	0-3	17820	-1.2	1.5	1.9	0.996
	SC	3-6	15120	-4.5	3.2	5.6	0.954
$TIGR_{1761}$	SW	0-6	950940	0.0	0.6	0.6	0.999
	SC	0-6	950940	-1.1	1.7	2.0	0.996
	SC	0-3	886680	-0.8	0.9	1.2	0.999
	SC	3-6	58860	-4.0	3.5	5.4	0.957
$TIGR_{2311}$	SW	0-6	249588	0.4	1.0	1.1	0.999
	SC	0-6	249588	-2.2	3.7	4.3	0.981
	SC	0-3	186732	-1.0	1.1	1.5	0.998
	SC	3-6	54216	-4.5	4.6	6.5	0.936
STD_{66}	SW	0-6	35640	-0.2	0.9	0.9	0.998
	SC	0-6	35640	-2.1	2.6	3.3	0.989
	SC	0-3	28080	-1.2	1.2	1.7	0.997
	SC	3-6	7020	-4.7	2.3	5.4	0.961

SW RMSEs are around 1 K, with a zero bias

ALGORITHMS

Testing from independent simulated data

Testing from independent simulated data

- TIGRs and STD databases
- 108 emissivity spectra (ASTER library)

Database	Algorithm	W range ($g \cdot cm^{-2}$)	n data	Bias (K)	St. Dev. (K)	RMSE (K)	r
$TIGR_{61}$	SW	0-6	32940	-0.1	1.2	1.2	0.997
	SC	0-6	32940	-2.7	3.0	4.0	0.982
	SC	0-3	17820	-1.2	1.5	1.9	0.996
	SC	3-6	15120	-4.5	3.2	5.6	0.954
$TIGR_{1761}$	SW	0-6	950940	0.0	0.6	0.6	0.999
	SC	0-6	950940	-1.1	1.7	2.0	0.996
	SC	0-3	886680	-0.8	0.9	1.2	0.999
	SC	3-6	58860	-4.0	3.5	5.4	0.957
$TIGR_{2311}$	SW	0-6	249588	0.4	1.0	1.1	0.999
	SC	0-6	249588	-2.2	3.7	4.3	0.981
	SC	0-3	186732	-1.0	1.1	1.5	0.998
	SC	3-6	54216	-4.5	4.6	6.5	0.936
STD_{66}	SW	0-6	35640	-0.2	0.9	0.9	0.998
	SC	0-6	35640	-2.1	2.6	3.3	0.989
	SC	0-3	28080	-1.2	1.2	1.7	0.997
	SC	3-6	7020	-4.7	2.3	5.4	0.961

SC algorithm fails for moderate to high *w* values
RMSE 3-4 K

ALGORITHMS

Testing from independent simulated data

Testing from independent simulated data

- TIGRs and STD databases
- 108 emissivity spectra (ASTER library)

Database	Algorithm	W range (g·cm^{-2})	n data	Bias (K)	St. Dev. (K)	RMSE (K)	r
$TIGR_{61}$	SW	0-6	32940	-0.1	1.2	1.2	0.997
	SC	0-6	32940	-2.7	3.0	4.0	0.982
	SC	0-3	17820	-1.2	1.5	1.9	0.996
	SC	3-6	15120	-4.5	3.2	5.6	0.954
$TIGR_{1761}$	SW	0-6	950940	0.0	0.6	0.6	0.999
	SC	0-6	950940	-1.1	1.7	2.0	0.996
	SC	0-3	886680	-0.8	0.9	1.2	0.999
	SC	3-6	58860	-4.0	3.5	5.4	0.957
$TIGR_{2311}$	SW	0-6	249588	0.4	1.0	1.1	0.999
	SC	0-6	249588	-2.2	3.7	4.3	0.981
	SC	0-3	186732	-1.0	1.1	1.5	0.998
	SC	3-6	54216	-4.5	4.6	6.5	0.936
STD_{66}	SW	0-6	35640	-0.2	0.9	0.9	0.998
	SC	0-6	35640	-2.1	2.6	3.3	0.989
	SC	0-3	28080	-1.2	1.2	1.7	0.997
	SC	3-6	7020	-4.7	2.3	5.4	0.961

SC algorithm fails for moderate to high *w* values

When Atmospheric profiles with *w* values lower than 3 g·cm^{-2} are selected, the SC algorithm provides RMSEs around 1.5 K

STUDY AREA AND DATA

Test sites

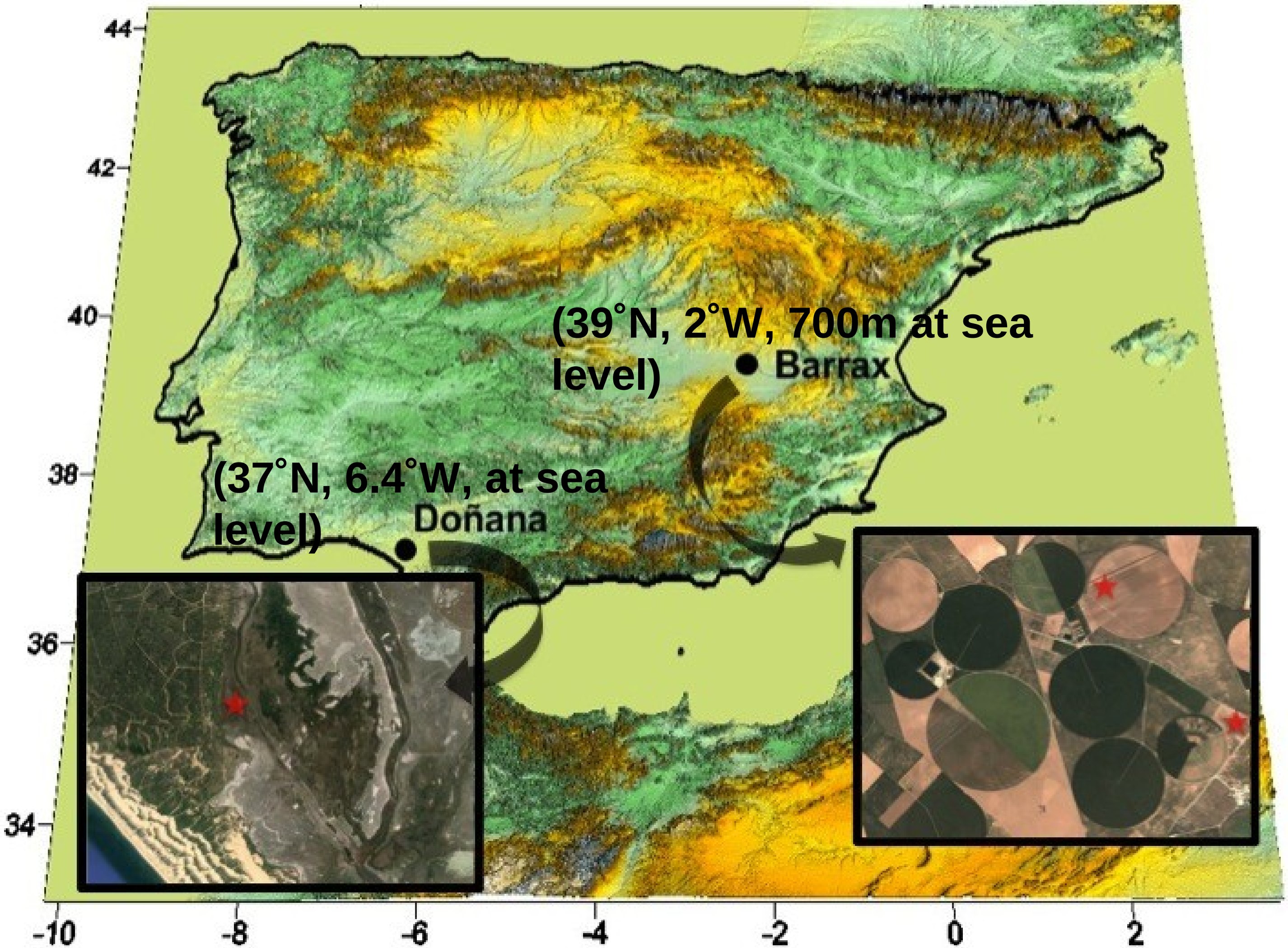

STUDY AREA AND DATA

Test sites

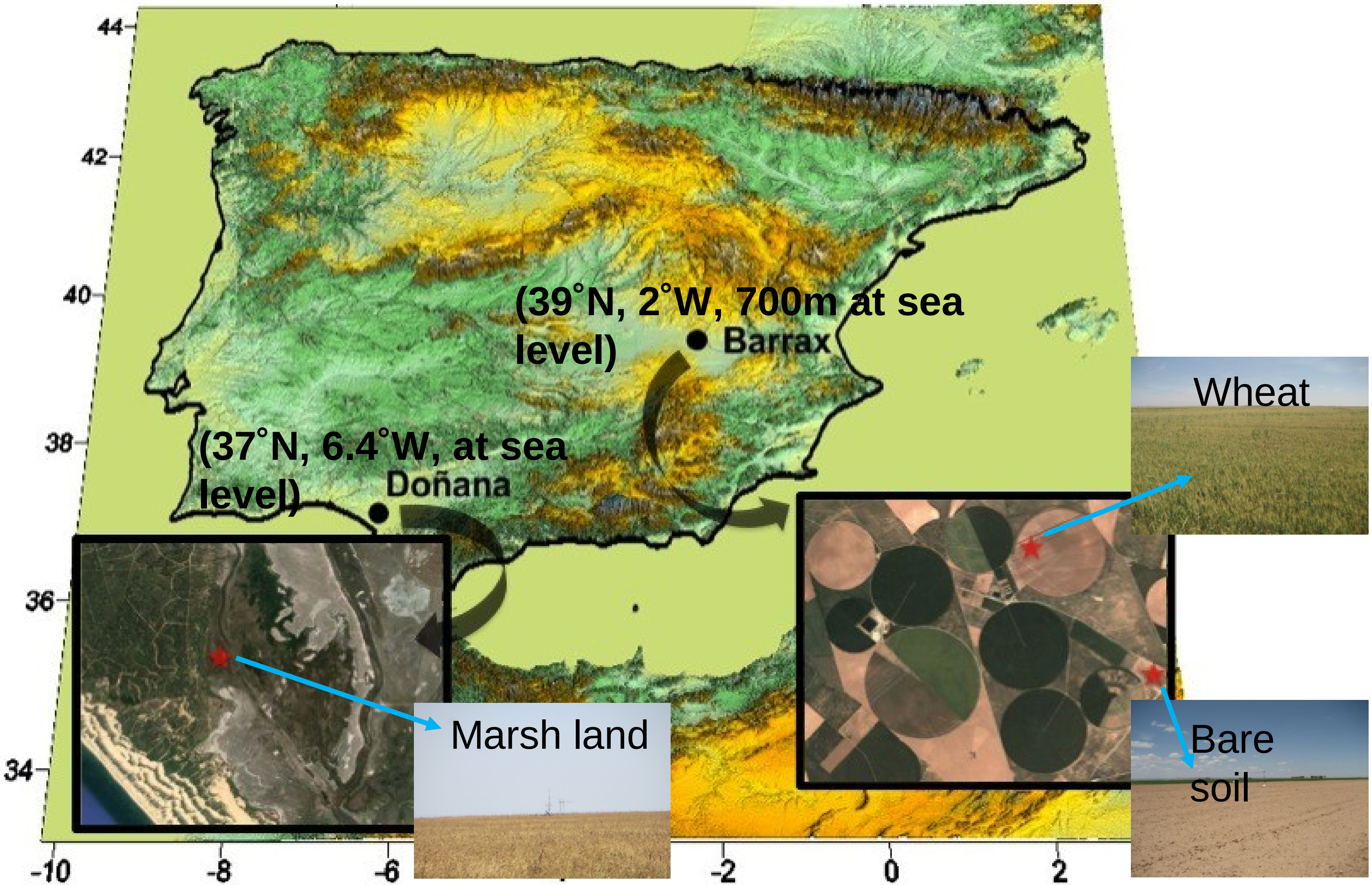

STUDY AREA AND DATA

Instruments

RADIOMETER IR120

OPTRIS CT-LT15

CIMEL CE312-1 & 2

IR120 & OPTRIS

- Single broadband (8-14 μm) radiometers

CIMEL CE3122

- Multiband radiometer
  - One broadband (8-14 mm)
  - Five narrowbands similar to the ASTER TIR bands

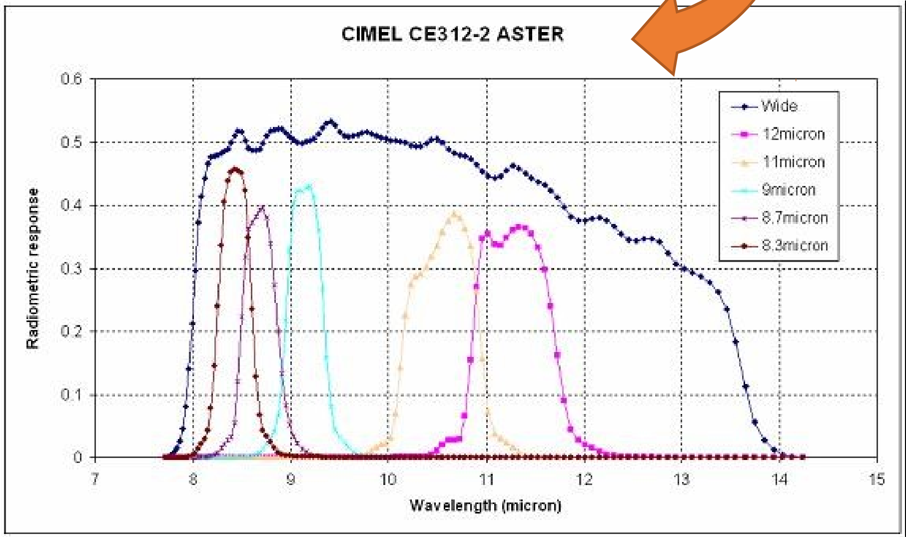

STUDY AREA AND DATA

Landsat data

- Five images
  - 2 Doñana (19 April 2013 and 5 May 2013)
  - 3 Barrax (1 June 2013, 24 June 2013, and 12 September 2013)

- OLI/VNIR bands:
  - Atmospheric correction based on the Dark Object Subtract (DOS) was performed.
  - NDVI obtained with bands 5 (NIR) and 4 (red)

- TIRS bands:
  - Atmospheric correction performed with MOD07 product.
  - Atmospheric parameters (w, τ, L_u, L_d) obtained with MODTRAN-4.
  - LST estimated with algorithms presented previously.

RESULTS

Vicarious calibration

- Significant bias (around 3 K) between Landsat-8 derived data and measured values of LST.
- Result later confirmed by the announcement published in the USGS Landsat mission web page on September 16, 2013.
- 2 points for calibration (extreme data points, the lowest and highest radiance)

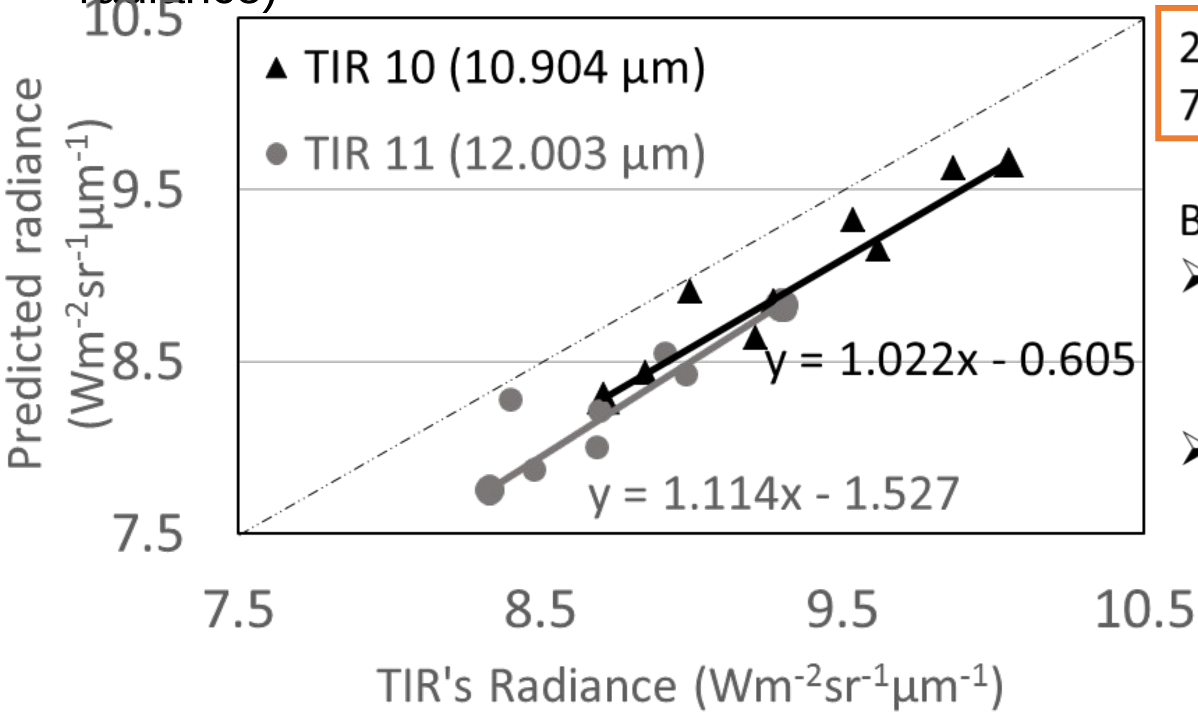

2 points for calibration
7 points for validation

Bias estimated at 300 K.

- TIRS 1 negative bias: ~0.4 $W \cdot m^{-2} \cdot sr^{-1} \cdot \mu m^{-1}$ ~2.6 K
- TIRS 2 negative bias: ~0.6 $W \cdot m^{-2} \cdot sr^{-1} \cdot \mu m^{-1}$ ~4.8 K

RESULTS

Intercomparison of algorithms

Results for the algorithms described above for ground-based measurements

Site	Date	W (g/cm²)	Plot	LST_{situ} (K)	LST_{RTE} (K)	LST_{SW} (K)	LST_{SC} (K)	D_{RTE} (K)	D_{SW} (K)	D_{SC} (K)
				Calibration Points						
Barrax	23/05	1.1	Wheat	291.8	-	-	-	-	-	-
Doñana	22/06	3.2	Marsh	304.7	-	-	-	-	-	-
				Validation Points						
Barrax	01/06	1.0	Wheat	292.8	292.3	291.4	292.4	-0.5	-1.4	-0.3
	24/06	1.4	Wheat	303.8	303.3	302.3	303.7	-0.4	-1.5	-0.1
	12/09	1.8	Corn	295.1	296.1	295.5	295.9	1.0	0.4	0.8
	12/09	1.8	Soil	301.1	301.0	300.0	300.8	-0.1	-1.0	-0.3
	12/09	1.8	Soil	302.6	301.8	301.6	301.6	-0.8	-1.0	-1.0
Doñana	19/04	2.0	Marsh	297.6	296.4	298.0	295.1	-1.2	0.4	-2.5
	05/05	1.7	Marsh	297.6	298.1	297.8	297.6	0.5	0.2	0.0
							Bias	-0.2	-0.6	-0.5
							SD	0.8	0.8	1.0
							RMSE	0.8	1.0	1.2

RESULTS

Intercomparison of algorithms

Similar results provided by all the LST methods:

Low and negative BIAS (-0.6 K)
Standard deviation around 1 K
RMSE lower than 1.5 K

Site	Date	W (g/cm^2)	Plot	LST_{situ} (K)	LST_{RTE} (K)	LST_{SW} (K)	LST_{SC} (K)	D_{RTE} (K)	D_{SW} (K)	D_{SC} (K)
Calibration Points										
Barrax	23/05	1.1	Wheat	291.8	-	-	-	-	-	-
Doñana	22/06	3.2	Marsh	304.7	-	-	-	-	-	-
Validation Points										
Barrax	01/06	1.0	Wheat	292.8	292.3	291.4	292.4	-0.5	-1.4	-0.3
	24/06	1.4	Wheat	303.8	303.3	302.3	303.7	-0.4	-1.5	-0.1
	12/09	1.8	Corn	295.1	296.1	295.5	295.9	1.0	0.4	0.8
	12/09	1.8	Soil	301.1	301.0	300.0	300.8	-0.1	-1.0	-0.3
	12/09	1.8	Soil	302.6	301.8	301.6	301.6	-0.8	-1.0	-1.0
Doñana	19/04	2.0	Marsh	297.6	296.4	298.0	295.1	-1.2	0.4	-2.5
	05/05	1.7	Marsh	297.6	298.1	297.8	297.6	0.5	0.2	0.0
							Bias	-0.2	-0.6	-0.5
							SD	0.8	0.8	1.0
							RMSE	0.8	1.0	1.2

RESULTS

Intercomparison of algorithms

Two images are selected

Barrax (23 May 2013)
Doñana (22 June 2013)

Direct inversion of the RTE is assumed to be a “ground-truth” reference.

Differences between the LST retrieved from SC and SW algorithms and LST retrieved from inversion of the RTE where analyzed.

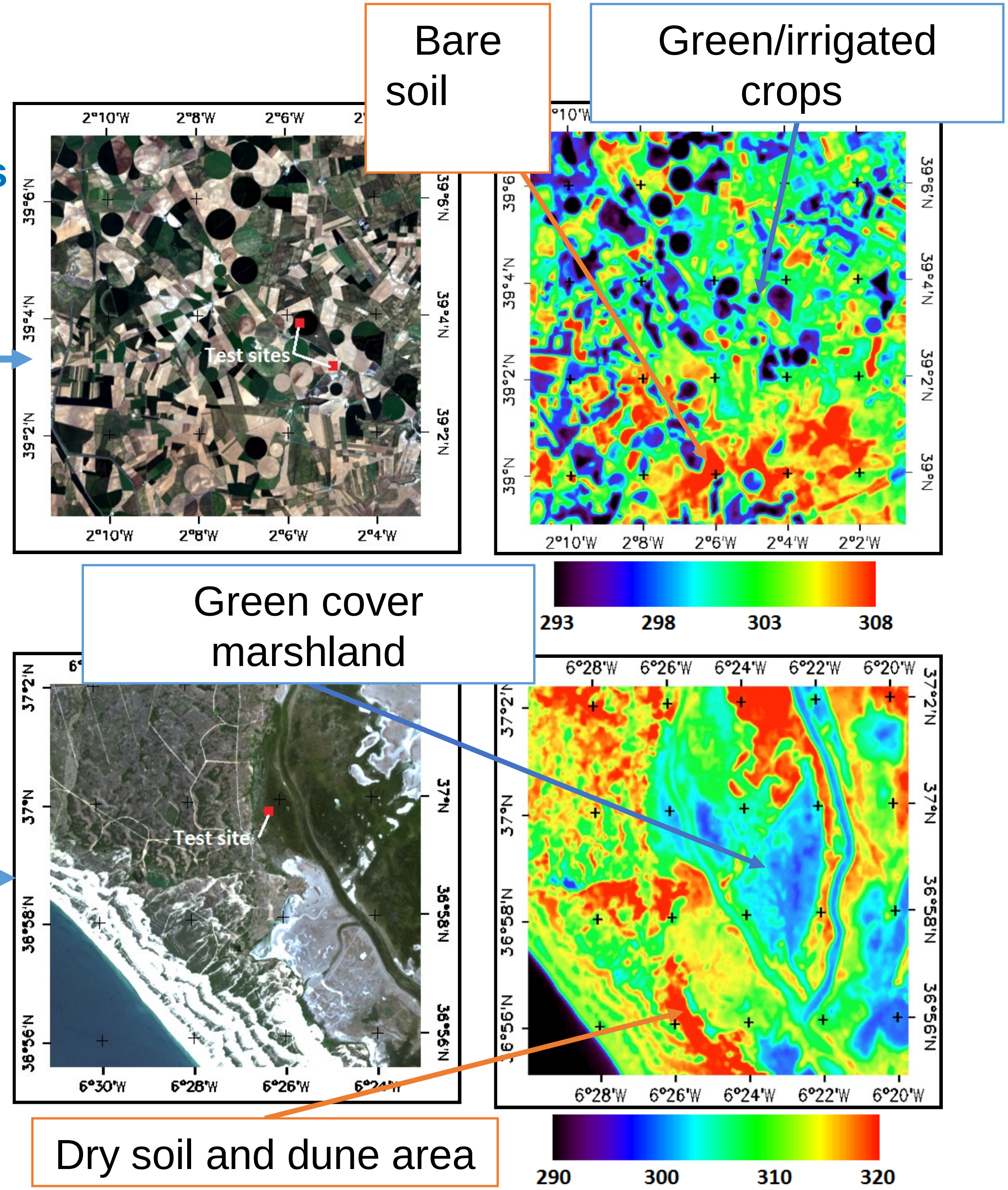

RESULTS

Intercomparison of algorithms

w = 1.0 $g \cdot cm^{-2}$	Barrax	
	LST_{SW}-LST_{RTE} (K)	LST_{SC}-LST_{RTE} (K)
Bias	0.10	0.14
SD	0.44	0.02
RMSE	0.45	0.14

BARRAX TEST SITE

- Similar bias for both algorithms
- Great standard deviation in SW algorithm

D_{RTE-SW} (K)

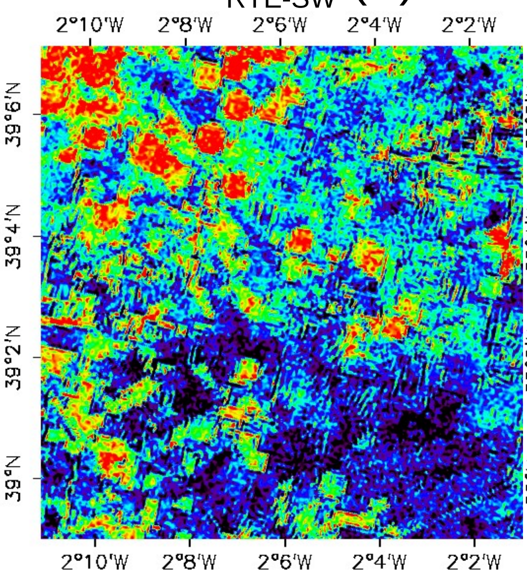

D_{RTE-SC} (K)

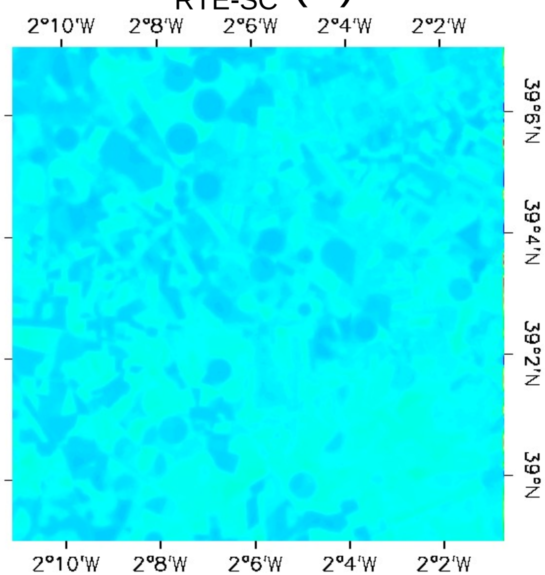

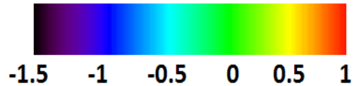

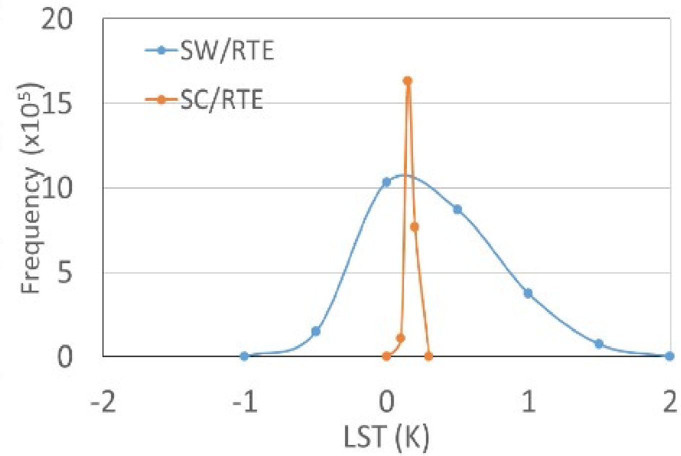

RESULTS

Intercomparison of algorithms

w = 3.2 g·cm^{-2}	Doñana	
	LST_{SW}-LST_{RTE} (K)	LST_{SC}-LST_{RTE} (K)
Bias	0.82	1.20
SD	0.61	0.28
RMSE	1.02	1.23

DOÑANA TEST SITE

- Greater BIAS in SC algorithm
- Great standard deviation in SW algorithm

$D_{RTE\text{-}SW}$ (K) $D_{RTE\text{-}SC}$ (K)

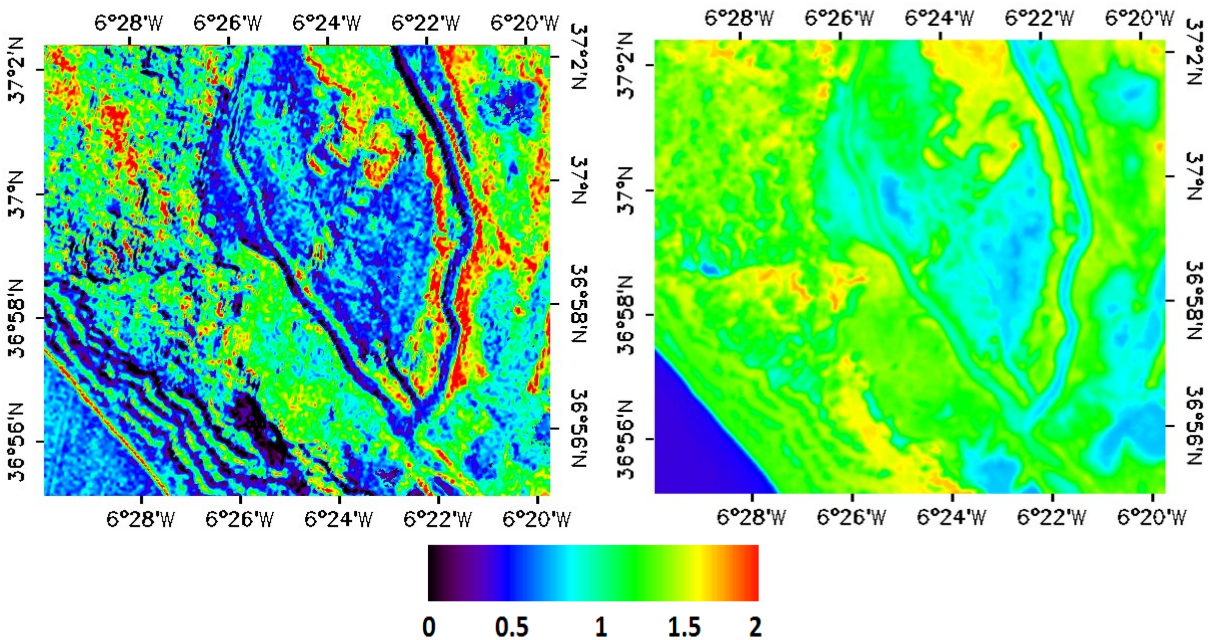

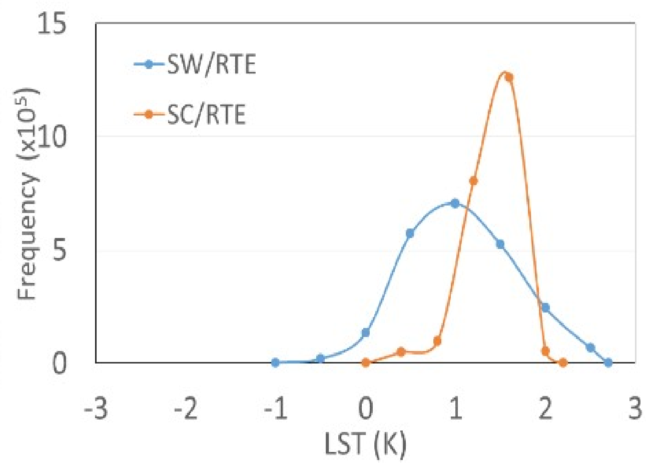

RESULTS

Intercomparison of algorithms

- RMSE are lower over Barrax <0.5 K than over Doñana, and in all cases below <1.3 K.
- Differences in RMSE could be explained by the different W values over the two sites, < 1 g·cm^{-2} for Barrax and near 3.5 g·cm^{-2} for Doñana.

BARRAX:
w = 1.0 g·cm^{-2}
RMSE < 0.5 K

DOÑANA:
w = 3.2 g·cm^{-2}
RMSE < 1.3 K

- Difference between temperatures at bands TIRS-1 and TIRS-2 also indicated a kind of miss-registration problem between the two TIR bands that can be observed in the image difference between SW and inversion of the RTE.

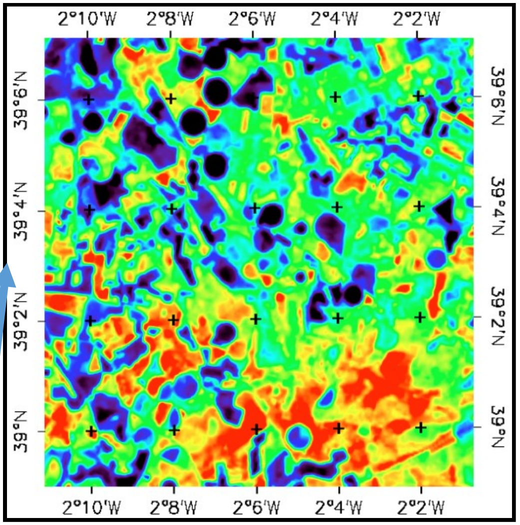

RT
E

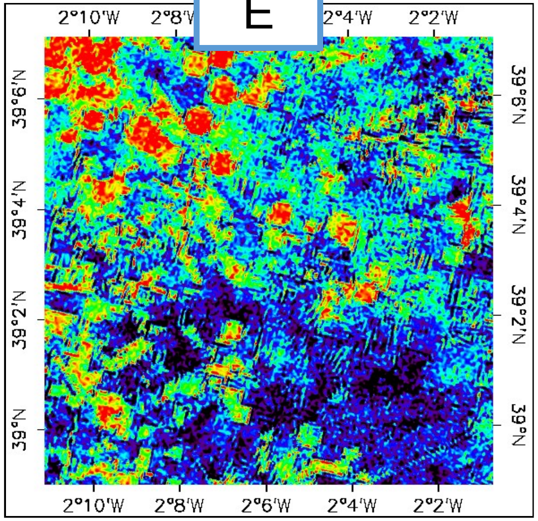

RTE-

Conclusions

- A SC and SW algorithm were presented to retrieve a LST with the new Landsat-8 TIRS bands with different physical assumptions.
- Advantage of the SC and SW algorithm are that only water vapor content and LSE are required as input.
- The application of LST algorithms to Landsat-8 imagery and the subsequent comparison of retrieved LST against *in situ* measurements revealed a significant bias (~3 K) that was corrected with a vicarious calibration (~0.4 and ~0.6 $W \cdot m^{-2} \cdot sr^{-1} \cdot \mu m^{-1}$ to TIRS 1 and 2 respectively) over our test sites.
- Comparing ground-based measurements with LST values retrieved with all the algorithms, a RMSE lower than 1.5 K was obtained. This result also agrees with a validation exercise performed for an extensive simulated dataset.
- SW errors are lower than SC errors for increasing water vapour, and vice versa.
- The validation results should be considered preliminary pending of more acquisitions over the test sites using the permanent stations managed by the Global Change Unit (University of Valencia) and the Spanish CEOS-Spain project sites.

Acknowledgements

- Instituto Técnico Agronómico Provincial (ITAP)
- Reserva Biológica de Doñana (RBD)
- NASA and the U.S. Geological Survey (USGS)
- Ministerio de Economía y Competitividad:
  - CEOS-Spain, project AYA2011-29334-C02-01)
- Program U-INICIA VID 2012 (grant U-INICIA 4/0612) from University of Chile